
Article:
Pal, P, Kumi-Barimah, E, Dawson, B et al. (2022) Manufacturing of Er-doped planar waveguides on silica-on-silicon using femtosecond laser-induced plasma. Optics Communications, 522. 128614. ISSN: 0030-4018

https://doi.org/10.1016/j.optcom.2022.128614

Manufacturing of Er^{3+}-doped planar waveguides on Silica-on-Silicon using Femtosecond Laser-Induced Plasma

Paramita Pal, Eric Kumi-Barimah, Benjamin Dawson, Gin Jose

School of Chemical and Process Engineering, University of Leeds, Clarendon Road, Leeds LS2 9JT, United Kingdom

Corresponding author: e.kumi-barimah@leeds.ac.uk

Abstract

We report fabrication and characterisation of the erbium-doped planar waveguide on a silica-on-silicon (SOS) wafer- offering low loss and strong light confinement suitable for engineering optical waveguide amplifier for the C-band (1530-1565 nm) of the optical fibre communication. Here we describe an ultrafast laser plasma doping (ULPD) technique that is carried out using the plasma induced by a femtosecond laser (wavelength 800 nm) with a repetition rate of 10 kHz and a pulse duration of 45 fs. The ULPD method presented here had been applied successfully for rare earth materials doping on SOS substrates previously using a fs-laser with a pulse duration of ~ 100 fs and at a repetition rate of 1 kHz. The fabricated planar optical waveguide layer onto the SOS substrate has been analysed for thickness, refractive index, optical propagation loss, photoluminescence intensity, and photoluminescence lifetime. We report a low propagation loss of <0.4dB/cm in the C-Band, a long lifetime of 13.21 ms at 1532 nm, and the largest lifetime-density product 6.344 $x10^{19}$ $s.cm^{-3}$. The low loss planar slab waveguide and a high lifetime-density product promise the further possibility of fabricating strip-loaded waveguides on the SOS platform. The proposed active waveguide fabrication methodology is potentially useful for manufacturing planar integrated optical waveguide amplifiers and lasers compatible with silicon-based photonic integrated circuits.

***Keywords*: Erbium-doped waveguide amplifier, femtosecond laser, pulsed laser deposition, silica-on-silicon**

Introduction

Silicon photonic integrated circuits (PICs) have attracted wide-range applications, including arrayed waveguide gratings, low power modulators, ultra-wideband multiplexers, waveguides for supercontinuum generation, and integrated quantum optics [1-6]. Such progress on silicon photonic platforms (e.g. silica, silica-on-silicon (SOS), and silicon-on-insulator) is attributed to the shortcomings of the bandwidth from electrical interconnects and improvements in microelectronic technologies that enable the integration of multiple optical functionalities onto a single on-*chip*-based platform. The silica and SOS platforms exhibit excellent wide bandwidth, low power consumption, and low optical loss of 0.1-0.3dB/cm in the visible and near-infrared region [7,8]. While the refractive index of silica or SOS matches with silica optical fibre, thus curtailing coupling losses. More importantly, silicon photonic platforms are compatible with mature complementary-metal-oxide-semiconductor manufacture technologies that enable high-volume optoelectronic device fabrication at a very low-cost [9].

Numerous demonstrations of silicon-based photonic components have been demonstrated, such as integrated modulators, light detectors, couplers, splitters, and resonators [10, 11]. Despite these successes, significant challenges hampered using bare silicon photonic platforms as gain media for optical waveguide amplifiers and light source generation (laser) applications due to their indirect bandgap and associated low emission quantum efficiency [12]. Consequently, doping these silicon

photonic platforms with light-emitting luminescent materials can provide luminous properties for engineering light amplifiers and laser sources. Thus, several promising technologies have been developed to dope or deposit light emit materials on/onto silicon photonic platforms to overcome such a drawback. For instance, on-chip hybrid integration or direct deposition of III-V semiconductor materials [13-17], rare earth (e.g. erbium (Er^{3+})) doped materials[18], and germanium (Ge) [20-22] on/onto silica and SOS are studied to realise optical components such as integrated laser sources, optical waveguide amplifiers, and photodetectors. Among these doping techniques, Er^{3+} doped host materials have long been demonstrated for laser sources and amplifications on silicon photonic platforms [23-24] to exploit its $^4I_{13/2} \rightarrow {}^4I_{15/2}$ radiative transition centred at 1534 nm. This transition corresponds to low loss and low-dispersion wavelengths lying in the telecommunication C-band (1525-1565 nm) and L (1565–1610 nm) bands [25-28] of silica. However, doping of rare-earth ions in silicon was unsuccessful in realising a practical device due to their poor light-emitting properties at room temperature and low lifetime-density product [7-12].

Various fabrication techniques have been reported to fabricate Er^{3+} ions doped silica or SOS platforms for optical waveguide amplifiers and lasers. These include reactive RF ion magnetron co-sputtered, plasma-enhanced chemical vapour deposition, ion implantation, nanosecond pulsed laser deposition (ns-PLD), and femtosecond pulsed laser deposition (fs-PLD) [18, 29]. The RF sputtering, ion implantation, and plasma-enhanced chemical vapour deposition are disadvantages in many applications due to the formation of cracks, the clustering of rare-earth ions in the films, low doping concentration of Er^{3+} ions, and consequently low optical gain. In contrast, the ULPD technique has emerged as a powerful technique for doping high-quality thin film on silica and SOS with a high Er^{3+} ion doping concentration [18, 30]. For instance, Chandrappan et al. [18] reported on the incorporation of various concentrations of Er^{3+}-ions into silica substrates at a temperature of 700 ^oC and a deposition chamber pressure of 70 mTorr by using fs-laser (centre wavelength ~800 nm, repetition rate -1.0 kHz, and pulsed width ~100 fs). The Er^{3+} modified silica glass thus prepared using the ULPD exhibited photoluminescence (PL) properties such as an intense PL emission with an emission peak centred at 1534 nm, long PL lifetimes spanning 10 to 13.2 ms, and a lifetime-density product of 0.96 x 10^{19} $s.cm^{-3}$. Similarly, Kamil et al. [30] also modified SOS substrates with Er^{3+} doped tellurite glass by using the plasma-assisted technique reported by Chandrappan et al. [18]. They demonstrated long PL lifetimes ranging from 10.79 ms to 12.29 ms of the Er^{3+}-ion-doped layer on the SOS substrate by employing three fs-laser fluences to ablate the target. These initial results demonstrate that the ULPD technique has considerable potential for doping rare-earth ions onto silicon photonic platforms with high concentrations of rare-earth ions, which overcomes the limitations encountered with the aforementioned conventional fabrication techniques. The UPLD process involves the ablation of the target material with fs-laser pulses, followed by the generation of a plasma plume consisting of energetic nanoparticle species of the target material (near-stoichiometric materials of the target), which expands at a high velocity and temperature. The plasma plume comprises nanoparticles that accelerate toward the substrate and then modify the substrate surface to form a homogeneous thin film through a thermal-assisted diffusion process. The ULPD technology has shown potential for realising short compact waveguide lasers and optical waveguide amplifiers on-chip with a high optical gain.

In this study, we report on the fabrication of Er^{3+} -doped tellurite glass modified silica (EDTS) planar waveguides on SOS substrate by employing a high repetition rate of 10 kHz fs-laser with a pulse width of 45 fs as a function of the laser fluence. The cross-section, thickness and refractive index, planar waveguide propagation loss, PL, lifetime, and lifetime-density product characteristics were investigated. The low propagation loss of the planar waveguide and their excellent PL properties are promising for engineering optical waveguide amplifiers and laser applications at 1.5 μm.

Experimental Details

Er^{3+}-ion-doped zinc-sodium-tellurite (TZN) glass used as the ablation target was prepared using the two-step process, which includes melting and quenching steps to form glass with a molar composition of $79.75TeO_2$–$10ZnO$-$10Na_2O$-$0.25Er_2O_3$,. The Er^{3+} ion density in the glass was $4.735x10^{21}$ ions/cm^3. The high purity (>99.99%) analytical grade oxide and carbonate chemicals were utilised to synthesise 25g batch weights with a similar preparation procedure reported elsewhere [18, 30]. The prepared Er^{3+} doped tellurite glass was finely polished for laser ablation experiments using a KMLabs Wyvern^{TM}-1000-10 femtosecond laser with centre wavelength, pulse repetition rate and pulse duration of 800 nm, 10 kHz, and 45 fs respectively. The laser comprised of Ti: sapphire chirped-pulse cryogenic regenerative amplifier system, a diode-pumped solid-state laser (Opus 532) oscillator, and a 532 nm Nd^{3+}:YAG laser (LDP-200MQG, Lee Laser). The spot size of the fs-laser on the target surface was ~8.5 $x10^{-5}$ cm^2. A commercially available SOS substrate obtained from Inseto (UK) Limited of size 30 mm (L) x 20 mm(W) x 630 µm was first cleaned with de-ionized water at a temperature of 50 °C, followed by acetone and isopropanol for 15 min, and then dried with clean lens tissue. The Er-TZN target material and SOS substrate were mounted in their respective holders in a customised vacuum chamber (PVD Products, USA). The distance between the substrate and the target material was 70 mm. The vacuum chamber was then pumped down to the base pressure of 10^{-6} Torr and then brought to 70 mTorr with high purity oxygen as an ambient gas throughout the sample preparation process. The substrate temperature was kept at 600°C, while the target was ablated with laser fluences of 0.44J/cm^2 (S1), 0.53J/cm^2 (S2) and 0.66 J/cm^2 (S3) for 4-hours at each laser fluence to prepare three samples. Subsequently, the vacuum chamber was allowed to cool down to room temperature before removing the fabricated sample.

The cross-section and elemental composition of sample S3 (the thickest of the three samples) were examined by focused ion beam (FIB- FEI Helios G4 CX DualBeam**)** and high-resolution transmission electron microscopy (HR-TEM-FEI Tecnai TF20) via scanning of transmission electron microscopy (STEM) and energy-dispersive X-ray spectroscopy (EDS). The refractive index and film thickness of the sample S3 were measured with a Metricon's Model 2010/M prism coupler with a laser source of wavelength 633 nm and 1310 nm for TE polarisation mode. The waveguide propagation loss at these wavelengths was measured by coupling the laser to the fundamental mode (TE0). The refractive index of all three samples fabricated was also measured by spectroscopic ellipsometry (Woollam M2000XI) for comparison. The surface roughness of the samples were measured using profilometry(XXXX). The down-conversion PL emission and lifetime of Er^{3+} ion centred at ~1530 nm were measured by employing an FS920 Spectrofluorimeter (Edinburgh Instruments, UK) for all three samples prepared. The Er^{3+}-doped-TZN modified SOS thin film samples were excited with a 980 nm semiconductor laser diode powered by a benchtop diode laser controller (LDC4005, Thorlabs Inc.).

Results and discussions

Figure 1 (a) illustrates a multi-layer TEM micrograph cross-section of sample S3 prepared using FIB-FEI Helios G4 CX DualBeam equipment. The cross-sectional analysis of the films confirms the formation of an Er^{3+} ion-doped tellurite glass modified silica (EDTS) layer with the undoped silica and silicon, which are distinguishable. The thickness of the EDTS layer was 1.334 µm. In comparison, the initial silica layer thickness of 3.0 µm decreased to 2.480 µm after the doping via thermal assisted diffusion of fs-laser induced plasma of Er^{3+} -doped tellurite glass target into the silica layer. High angle annular dark-field (HAADF) cross-sectional STEM image was utilised for energy-dispersive X-ray spectroscopy (EDS) analysis of the as a grown layer. Figure 1 (b) shows a uniform and homogeneous distribution of elements Si, Er, Na, Zn and Te throughout the entire cross-section of the EDTS layer. The five chemically distinct EDS mappings correspond to the silica and EDTS layer.

Furthermore, the spatial distributions of the various constituent elements across the EDTS layer (sample S3) were obtained using an EDS line-scan profiling analysis, as shown in Figure 1(c). The section marked by the dash lines represents the boundaries of the EDTS layer. The elemental signals for Si, Te, Zn, Na, and Er are homogeneously distributed across the measured thickness of the EDTS layer. From the EDS-line-scan profile, the Si and Te are comparatively higher on both the top and bottom of the EDTS layer, representing the silica layer being the host material and a higher nominal concentration of Te in the target glass composition. This clearly shows that the Er^{3+} -doped tellurite glass elements are intermixed with a top portion of the SOS, as shown in Fig 1 (b), resulting in the modified layer expanding to the pristine silica layer.

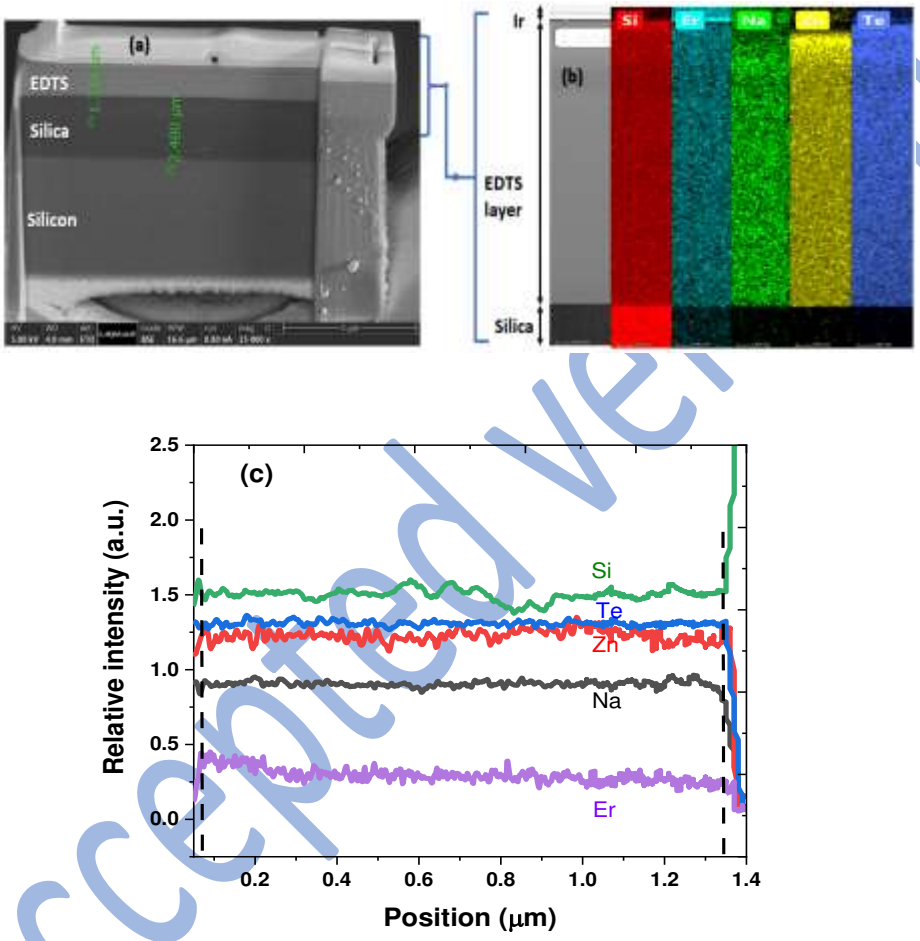

Figure1: (a) TEM cross-sectional image of EDTS buffered on-silicon thin film, the bright top layer is Ir metal coating used for preparation of the lamella (b) High angle annular dark-field (HAADF) cross-sectional image of S3 with STEM-EDS elemental colour mapping of silicon (Si), erbium (Er), Sodium (Na), zinc (Zn) and tellurium (Te), (c) EDX line scan profile of Er^{3+}-doped tellurite glass modified silica layer.

The refractive indices and thicknesses of the bare silica layer and EDTS buffered SOS substrate were initially measured by the spectroscopic ellipsometry method from the spectral range of 600 to 1200 nm. These measurements were carried out at room temperature with angles of incidence of 60 °, 65 °, and 75°. The real part refractive index was obtained by fitting Psi (ψ) and Delta (Δ) data point spectra with the Cauchy dispersion equation. Figure 2(a) illustrates the comparison between the refractive index curves of samples S1, S2, S3, and untreated silica layer-on-silicon in the wavelength range from 600 to 1200 nm. The real part refractive index was obtained by fitting Psi (ψ) and Delta (Δ) data point spectra with the Cauchy dispersion equation. The refractive indices thus obtained for samples S1 and S2 range from 1.61 to 1.55 in the wavelength range 600 to 1200 nm, as shown in Figure 2(a), whereas

sample S3 has a refractive index varying between ~1.66 and 1.64 in the same wavelength range. The film thicknesses obtained using ellipsometry were 0.480 µm, 0.571 µm, and 1.317 µm for samples S1, S2 and S3. The average surface roughness measured using surface profilometry (Bruker DektakXT stylus Profilometer) was found to be 14nm, 13.7 nm, and 10 for samples S1, S2 and S3 respectively. This clearly demonstrates that the refractive index and thickness of the EDTS layer increased substantially with increasing laser fluence to 0.66 J/cm2 compared to that prepared at lower fluences.

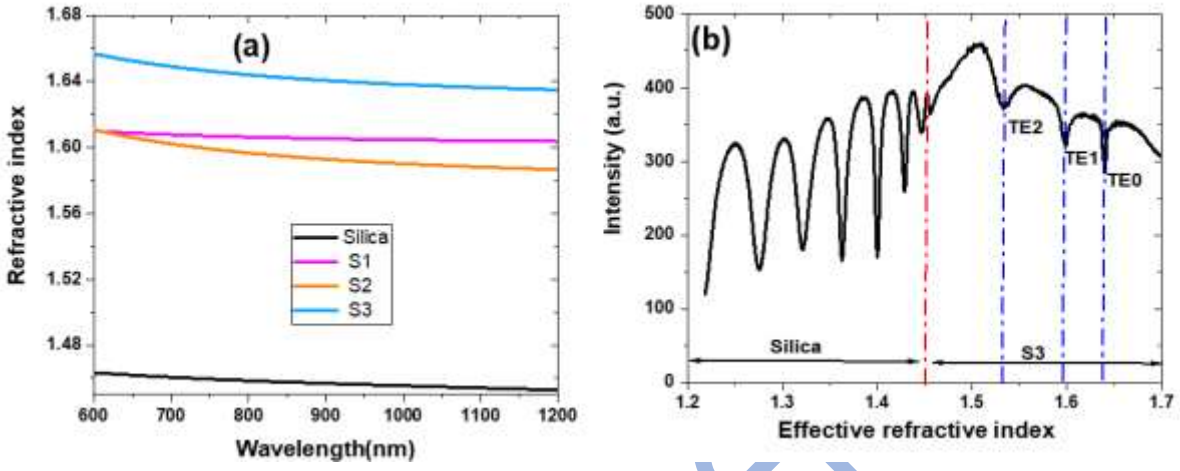

Figure 2: (a) Comparing refractive indices of the EDTS layer (sample S3) and untreated silica layer on-top of silicon measured by using ellipsometry (b) Prism coupler measurement with dips (marked blue on the right-hand side) in the curve corresponding to the guided modes of the waveguide and effective refractive indexes of sample S3. It also shows the radiation modes of the silica and silicon combined substrate directly beneath the EDTS layer. The red dot line approximately indicates the interface between the EDTS and silica layers.

Furthermore, a Metricon's prism coupler system was utilised to validate the film thicknesses and refractive indices of samples S1, S2 and S3. Figure 2(b) shows the guided modes obtained for sample S3 measured by prism coupler. The surface refractive index and film thickness at a wavelength of 633 nm were 1.654 and ~1.340 µm for sample S3, which correlates closely with the ellipsometry and TEM cross-sectional measurements. The refractive index obtained from the EDTS buffered-on-silicon samples are slightly higher than those reported previously[18]. Furthermore, the measurements revealed the effective indexes for three different guided modes occurring at TE0(1.6405), TE1 (1.6003) and TE2(1.5364) [shown in Figure 2(b)]. In contrast, the coupling of light from silica-on-silicon produced the radiation modes from which the refractive index and thickness of the silica layer are calculated as 1.4519 and 2.45 µm, respectively. However, we could not determine the guided modes for samples S1 and S2, owing to the low film thickness, which does not support guided modes at 633 nm.

In addition, the TE0 mode obtained from the EDTS planar waveguide was utilised to carry-out waveguide propagation loss measurements using a prism coupler. Propagation losses of 0. 51 ±0.02 dB/cm and 0.42±0.02 at 633 nm and 1310 nm wavelengths were obtained for the TE0 mode of a waveguide of length 1.63 cm for S3. From these measured values we can safely say the propagation loss in the C-band can be <0.4 dB/cm as the losses are expected to be lower at these wavelengths in silica/silicate glass-based waveguides. The optical loss result obtained from the fs-PLD fabrication technique is lower than Er^{3+} doped TeO_2 glass and siloxane polymer composite thin film deposited on silica substrate using excimer (193 nm) laser -PLD [31]. Here, a propagation loss of 1.03 dB/cm at 633 nm laser was reported for Er^{3+} doped TeO_2 glass and siloxane polymer composite thin film fabricated onto silica substrate at 100°C. It has been reported that propagation loss of rare earth ions

doped host materials such as TeO_2 and Al_2O_3 thin films deposited on silicon photonic substrates depends mainly on the deposition technique. For example, Suarez-Garcia et al. [32] reported a propagation loss of ~2.5 dB/cm at 632 nm on amorphous Al_2O_3 thin films grown on silicon substrate using an ArF laser beam (193 nm, 20 Hz). Similarly, a propagation loss of as low as ~0.4 dB/cm at 633 nm was reported using atomic layer deposition and reactive sputtering to fabricate Al_2O_3 thin films [33,34].

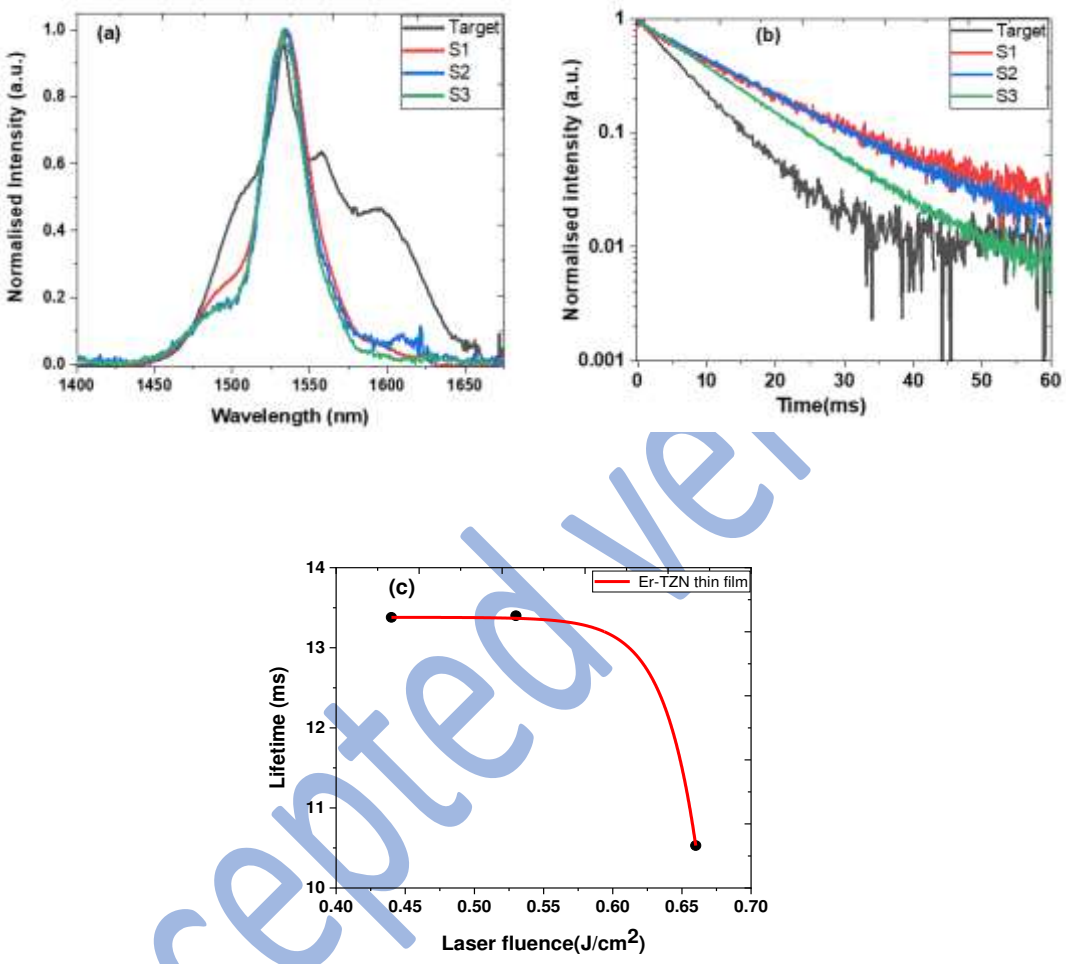

Figure 3: (a) Normalized PL spectra of the Er-TZN target glass and *EDTS* layer-on-silicon samples (S1, S2, and S3) at various laser fluences by excitation using a 980 nm semiconductor diode laser at room temperature. (b) PL decay curve for Er-TZN target and *EDTS* layer-on-silicon samples, (c)Fs-laser fluence dependence on the PL lifetime on the fabricated thin films

Figure 3 (a) illustrates normalised PL intensity spectra recorded for Er^{3+} -doped tellurite glass target and EDTS buffered SOS substrate at room temperature by employing a 980 nm semiconductor diode laser as an excitation source. The PL intensity peak centred at 1534 nm is assigned to the radiative transition of the Er^{3+} ions from the first excited state ($^4I_{13/2}$) to the ground state ($^4I_{15/2}$). The PL spectrum of Er^{3+} -doped tellurite glass target exhibits a full width at half-maximum (FWHM) of 71.8 nm. In contrast, the FWHM for EDTS buffered-on-silicon substrate samples S1, S2, and S3 are 36.50 nm, 33.48 nm, and 33.30 nm, respectively, decreasing slightly as the laser fluence increases. Thus, such a decrease in FWHM with increased laser fluence and EDTS film thickness is ascribed to an increase in Er^{3+} ions concentration, which leads to a high signal-to-noise ratio of the PL emission signal. On the other hand, the aforementioned EDTS films prepared using a 1.0 kHz femtosecond laser with high laser fluences and longer deposition time result in a thicker EDTS layer with a higher signal-to-noise

ratio and narrow emission intensity with short FWHM values than those samples reported elsewhere [18, 30]. In addition, Figure 3(b) illustrates the PL decay of the $^4I_{13/2}$ to $^4I_{15/2}$ transition level of the Er^{3+} -doped tellurite glass target and thin-film samples S1, S2 and S3 excited with a modulated 980 nm semiconductor laser. It is observed that the lifetime of ~13.40 ms was achieved for samples S1 and S2; nevertheless, this decreased by ~21% with increasing laser fluence to 0.66 J/cm^2 (sample S3), as depicted in Figure 3(c). The trend in the PL decay lifetime for the EDTS -SOS samples is shown graphically in Figure 3(b).

The decrease in PL lifetime at higher laser fluence can be ascribed to higher Er^{3+} ion concentrations in the doped layer, which leads to a reduced overall Er^{3+} - Er^{3+} ion spacing, which allows them to interact and transfer energy, leading to self-quenching of PL [34,35]. The figure-of-merit quantity known as a lifetime-density product for Er^{3+}-doped materials was adopted to determine the suitability for the EDTS layer for optical amplifiers and gain materials for compact laser applications. The EDTS layers show lifetime-density products ranging from 4.73 x 10^{19} s.cm^{-3} to 6.34 x 10^{19} s.cm^{-3} indicating a good material for applications of optical gain elements at around 1532 nm wavelength. These PL lifetime results are comparable to those samples fabricated previously via 1.0 kHz fs-laser with pulsed width of 100 fs and fs-laser fluences of 1.766 J/cm^2, 2.12 J/cm^2 and 2.83 J/cm^2 [30] where the PL lifetimes attained range from 10.76 to 12.29 ms, decreasing with high fs-laser fluences. Likewise, Chandrappan et. al.[18] reported lifetimes ranged from 10.0 to 13.2 ms and a lifetime density of 0.96 x 10^{19} s.cm^{-3} by depositing Er-doped TZN glass onto silica substrate using the 1.0kHz femtosecond laser.

Conclusion

In summary, a high repetition rate fs- laser (10 kHz) ULPD technique has been successfully utilised to deposit Er^{3+} -doped tellurite glass target into silica buffered-on-silicon substrate, increasing the growth rate of the thin film as compared to the samples fabricated previously by 1 kHz fs-laser. *EDTS* buffered-on-silicon waveguides exhibit a high refractive index of 1.654 and low propagation losses of <0.4dB/cm in the C-Band of fibre optics communication. Samples prepared at different fluences also have an average PL FWHM of 34.43nm with an accompanying PL lifetime range from 10.53 ms to 13.40 ms. This study concluded that a higher repetition rate fs-laser based ULPD is a promising technique for fabricating good quality rare-earth-doped planar waveguides on SOS with suitable excellent surface quality to engineer portable, low-cost optical waveguide amplifiers and lasers for the high-speed internet and data transmission applications, and for silicon PIC.

Declaration of Competing Interest

The authors declare that they have no known competing financial interests or personal relationships that could have appeared to influence the work reported in this paper.

Acknowledgement

The authors acknowledge the financial support from Engineering and Physical Sciences Research Council (EPSRC) for their financial support through the research Grants (EP/M015165/1, EP/T004711/1 and EP/M022854/1). Thanks to Mr John Harrington and Dr Zabeada Aslam at Leeds Electron Microscopy and Spectroscopy (LEMAS) Centre for the support in carrying out the TEM measurements. Benjamin Dawson acknowledges EPSRC DTP scholarship from the University of Leeds and NQIT Oxford.

References

[1] M. Kawachi, Silica waveguides on silicon and their application to integrated-optic components, Optical and Quantum Electronics, 22 (1990) 391–416.

[2] Syms R.R.A. (1994) Silica-on Silicon Integrated Optics. In: Martellucci S., Chester A.N., Bertolotti M. (eds) Advances in Integrated Optics. Springer, Boston, MA

[3] Q. Cheng, M. Bahadori, M. Glick, S. Rumley, Keren Bergman, Recent advancement in optical technologies for a data centre: review, Optica, 5(11) (2018) 1354-1369.

[4] J. Leuthold, C. Koos, C. Freude, Nonlinear silicon photonics, Nature Photon, 4(2010) 535-44.

[5] R. Van Laer, B. Kuyken, D. Van Thourhout, R. Baets, Interaction between light and highly confined hypersound in a silicon photonic nanowire, Nature Photon, 9 (2015) 199-203.

[6] J. Rönn, W. Zhang, A. Autere, X. Leroux, L. Pakarinen, C. Alonso-Ramos, A. Säynätjoki, H. Lipsanen, L. Vivien, E. Cassan , Z. Sun, Ultra-high on-chip optical gain in erbium-based hybrid slot waveguides, Nature Communications, 10 (2019) 432.

[7] H. Ou, Different index contrast silica-on-silicon waveguide by PECVD, Electron Letters, 39(2)(2003) 212-213 .

[8] Ozhikandathil, M. Packirisamy, Silica-on-silicon waveguides integrated polydimethylsiloxane lab-on-a-chip for quantum dot fluorescence bio-detection, Journal of Biomedical optics, 17(1) (2012) 017006.

[8] A. Politi, M. J. Cryan, J. G. Rarity, S. Yu, J. L. O'Brien, Silica-on-Silicon Waveguide Quantum Circuits, Science, 320, (2008) 646-649.

[9] Q. Xu, B. Schmidt, S. Pradhan, and M. Lipson, Micrometre-scale silicon electro-optic modulator, Nature, **4**35(7040) (2005) 325–327.

[10] G. Masini, L. Colace, G. Assanto, H. C. Luan, K. Wada, and L. C. Kimerling, High responsitivity near infrared Ge photodetectors integrated on Si," Electron. Lett. 35**(**17) (1999) 1467–1468.

[11] Zhou, Z., Yin, B. & Michel, J. On-chip light sources for silicon photonics. Light Sci Appl. 4 (2015) e358.

[12] G. Roelkens, D. Van Thourhout, R. Baets, R. Nötzel, and M. Smit, "Laser emission and photodetection in an InP/InGaAsP layer integrated on and coupled to a Silicon-on-Insulator waveguide circuit," Opt. Express, (18) (2006) 8154–8159.

[13] H. Park, Y. H. Kuo, A. W. Fang, R. Jones, O. Cohen, M. J. Paniccia, and J. E. Bowers, "A hybrid AlGaInAssilicon evanescent preamplifier and photodetector, Opt. Express 15(21) (2007) 13539–13546.

[14] A. W. Fang, H. Park, O. Cohen, R. Jones, M. J. Paniccia, and J. E. Bowers, "Electrically pumped hybrid AlGaInAs-silicon evanescent laser," Opt. Express 14(20) (2006) 9203–9210.

[15] J. V. Campenhout, P. R. Romeo, D. V. Thourhout, C. Seassal, P. Regreny, L. D. Cioccio, J.-M. Fedeli, and R. Baets, Design and optimization of electrically injected InP-based microdisk lasers integrated on and coupled to a SOI waveguide circuit, IEEE J. Lightwave Technol. 26(1) (2008) 52–63.

[16] M. Kapulainen, S. Ylinen, T. Aalto, M. Harjanne, K. Solehmainen, J. Ollila, and V. Vilokkinen, Hybrid integration of InP lasers with SOI waveguides using thermocompression bonding," in Proceedings of 5th IEEE International Conference on Group IV Photonics (Institute of Electrical and Electronics Engineers, New York, (2008), 61–63.

[17] K. Vu, S. Madden, Tellurium dioxide Erbium doped planar rib waveguide amplifiers with net gain and 2.8dB/cm internal gain, Optical Express, 18(18) (2010)19192-19200.

[18] J. Chandrappan, M. Murray, T. Kakkar, P. Petrik, E. Agocs, Z. Zolnai, D. P. Steenson, A. Jah, G. Jose, Target dependent femtosecond laser plasma implantation dynamics in enabling silica for high density erbium doping, Scientific Reports, 5:14037 (2015) 1-8.

[19] L. Chen, K. Preston, S. Manipatruni, and M. Lipson, Integrated GHz silicon photonic interconnect with micrometer-scale modulators and detectors, Opt. Express 17(17) (2009) 15248–15256.

[20] T. Yin, R. Cohen, M. M. Morse, G. Sarid, Y. Chetrit, D. Rubin, and M. J. Paniccia, 31 GHz Ge n-i-p waveguide photodetectors on Silicon-on-Insulator substrate, Opt. Express 15(21) (2007) 13965–13971.
[21] D. Ahn, C. Y. Hong, J. Liu, W. Giziewicz, M. Beals, L. C. Kimerling, J. Michel, J. Chen, and F. X. Kärtner, High performance, waveguide integrated Ge photodetectors, Opt. Express 15(7), 3916–3921 (2007).
[22] J. Kalkman, A. Polman, T. J. Kippenberg, K. J. Vahala, M.L. Brongersma, Erbium-implanted silica microsphere laser. Nucl. Instruments Methods Phys. Res. Sect. B Beam Interact. with Mater. Atoms 242, 182–185 (2006).
[23] H. Isshiki, T. Kimura, Toward small size waveguide amplifiers based on erbium silicate for silicon photonics. IEICE Trans. Electron. E91-C (2008) 138–144.
[24] S.Dai, C. Yu, G. Zhou, J. Zhang, G. Wang, L. Hu, Concentration quenching in erbium-doped tellurite glasses, Journal of Luminescence, 117(1) (2006) 39-45.
[25] R. Rolli, M.Montagna, S. Chaussedent, A. Monteil, V.K. Tikhomirov, M. Ferrari, Erbium-doped tellurite glasses with high quantum efficiency and broadband stimulated emission cross section at 1.5 µm, Optical Materials, 21(1) (2003) 743-748.
[26] E. A. Anashkina, Laser Sources Based on Rare-Earth Ion Doped Tellurite Glass Fibers and Microspheres, Fibers, (2020) 1-17
[27] C.E. Chryssou, F. Di Pasquale, & C.W. Pitt, Er^{3+}-doped channel optical waveguide amplifiers for WDM systems: A comparison of tellurite, alumina and Al/P silicate materials, IEEE Journal on Selected Topics in Quantum Electronics **6** (2000)114-121.
[28] S. Dai, C. Yu, G. Zhou, J. Zhang, G. Wang, & L. Hu, Concentration quenching in Erbium-doped tellurite glasses, Journal of Luminescence **117**, 39-45 (2006).
[29] S. Shen, W.H Chow, D. P. Steenson, A. Jha, Erbium-doped waveguide fabrication via reactive pulsed laser deposition of erbium-doped oxyfluoride-silicate glass, Electronic Letters 41(25) (2006) 1376-1377.
[30] A. Kamil, J. Chandrappan, M. Murray, P. Steenson, T. F. Krauss, G. Jose, Ultrafast laser plasma doping of Er^{3+} ions in silica-on-silicon for optical waveguiding applications, Optics Letters,41(20) (2016) 4684-4687.
[31] Z. Zhao , G. Josel , M. Irannejadl , P. Steenson , N. Bamiedakis , R. V Penty , I. H. White, A. Jha, Er3+ -doped Glass-polymer Composite Thin Films Fabricated Using Combinatorial Pulsed Laser Deposition, CLEO EUROPE/EQEC, 2011, DOI: 10.1109/CLEOE.2011.5942854.
[32] W.A.P. M Hendriks, et al. Low loss aluminium oxide with high refractive index. Proc ECIO. 2020
[33] A. Suárez-García, J. Gonzalo, C. N. Afonso, Low-loss Al_2O_3 waveguides produced by pulsed laser deposition at room temperature. Appl Phys A. 77 (2003) 779–783
[34] The role of Er^{3+}-Er^{3+} separation on the luminescence of Er-doped Al_2O_3 films prepared by pulsed laser deposition, Applied Physics Letters, 75(26) (1999) 4073-4075·
[35] K. S. Albarkaty, E. Kumi-Barimah, C. Craig, D. Hewak, G. Jose, J. Chandrappan, Erbium-doped chalcogenide glass thin film on silicon using femtosecond pulsed laser with different deposition temperatures, Applied Physics A, 125(1) (2019) 1-8.